

GPU-Accelerated Algorithms for Process Mapping

1st Petr Samoldekin
Heidelberg University
Heidelberg, Germany

2nd Christian Schulz
Heidelberg University
Heidelberg, Germany

3rd Henning Woydt
Heidelberg University
Heidelberg, Germany

Abstract—Process mapping asks to assign vertices of a task graph to processing elements of a supercomputer such that the computational workload is balanced while the communication cost is minimized. Motivated by the recent success of GPU-based graph partitioners, we propose two GPU-accelerated algorithms for this optimization problem.

The first algorithm employs hierarchical multisection, which partitions the task graph alongside the hierarchy of the supercomputer. The method utilizes GPU-based graph partitioners to accelerate the mapping process. The second algorithm integrates process mapping directly into the modern multilevel graph partitioning pipeline. Vital phases like coarsening and refinement are accelerated by exploiting the parallelism of GPUs.

In our experiments, both methods achieve speedups exceeding 300 when compared to state-of-the-art CPU-based algorithms. The first algorithm has, on average, about 10 percent greater communication costs and thus remains competitive to CPU algorithms. The second approach is much faster, with a geometric mean speedup of 77.6 and peak speedup of 598 at the cost of lower solution quality. To our knowledge, these are the first GPU-based algorithms for process mapping.

Index Terms—GPU, Process Mapping, Graph Partitioning.

I. INTRODUCTION

Parallel high-performance applications rely on the efficient execution of large numbers of tasks across massively parallel architectures. This involves placing individual tasks on the Processing Elements (PEs) of the underlying hardware architecture such that the computational workload is evenly balanced. However, load balancing alone is not sufficient. In parallel applications, the individual tasks usually communicate with each other, i.e., they send and receive data to and from each other. The cost of this communication heavily depends on the location of the tasks in hardware topology. Modern supercomputers are typically organized hierarchically, for example into processors, nodes, racks and islands. The communication cost between two PEs, therefore, depends on their relative locations within this hierarchy. Two PEs on the same processor communicate data much more quickly than two PEs which are located on different islands. Thus, in addition to balancing the workload, it is advantageous to minimize the total communication cost by placing highly interactive tasks close to each other. This optimization problem is known as the *general process mapping problem* (GPMP).

Optimally solving the GPMP is NP-hard [39] as it involves solving the well-known *quadratic assignment problem* (QAP) [9]. The QAP asks for a set of n facilities and n

locations to minimize the total cost of assigning each facility to one location, where the cost depends on both the flow between facilities and the distance between their locations. Since the QAP is strongly NP-hard, i.e., no constant factor approximation exists unless $P = NP$, its hardness transfers to the GPMP. The hardness is also reflected in practice as no meaningful instance with $n > 20$ can be solved in a reasonable time [9]. Moreover, the same hardness result arises from *graph partitioning* (GP), where the goal is to partition a graph while minimizing the number of edges between them. Graph partitioning is NP-complete and also admits no constant-factor approximation unless $P = NP$.

The GPMP is commonly solved using either the *two-phase* approach or via *integrated mapping*. In the two-phase approach, the task set is first partitioned into as many (almost) equally sized sets as there are PEs in the supercomputer. While partitioning the task set, the necessary communication between the resulting sets is minimized. In the second phase, the subsets are mapped to the PEs such that the total cost of communication is minimized, taking the distances between the PEs into account. The first phase is an instance of GP, while second phase is a QAP instance. The two-phase approach is often easier to realize as it can fall back to two well-studied problems, i.e., graph partitioning the QAP. The algorithm SHAREDMAP [44] currently offers state-of-the-art solution quality by utilizing *hierarchical multisection*, a special variant of the two-phase approach.

The integrated mapping approach combines both phases into a single process by incorporating the mapping objective directly into the graph partitioning pipeline. Rather than minimizing the number of edges crossing between the subsets, as in classical graph partitioning, it directly minimizes the total cost of communication. Typically, this is achieved using the modern multilevel framework, which involves coarsening the input graph to a smaller representation, computing an initial mapping, and then refining it during uncoarsening. The approach is more complex to realize as the whole graph partitioning pipeline has to be adopted to the new objective function. However, this also enables function specific optimization, which result in an overall faster execution time. As a result, integrated mapping often achieves faster runtimes compared to the two-phase approach.

Recently, Graphic Processing Units (GPUs) have been utilized to tackle graph partitioning. GPUs provide massive parallelism that can significantly reduce runtime, when exploited effectively. However, leveraging thousands of GPU cores is

Henning Woydt is funded by the Deutsche Forschungsgemeinschaft (DFG, German Research Foundation) – DFG SCHU 2567/6-1

challenging due to the irregularity of graphs and lack of straightforward parallelization strategies. Despite this, recent GPU-based algorithms like JET [18] and G-KWAY [31] have demonstrated promising results. They deliver solution qualities comparable to the serial CPU-based partitioner METIS [27], while being up to 20 times faster. Since both the two-phase and integrated mapping approach rely on graph partitioning, these results should transfer to GPMP.

Our Contribution. We present the first GPU-based approach to the process mapping problem, introducing two GPU-accelerated algorithms: a hierarchical multisection method and an integrated mapping variant. Both significantly outperform state-of-the-art CPU solvers in runtime, achieving speedups of more than 500 \times , while remaining competitive to the solution quality of CPU-based approaches.

II. PRELIMINARIES

A. Concepts and Notations

Let $G = (V, E)$ with $n = |V|$ and $m = |E|$ be an undirected graph, and let $c : V \mapsto \mathbb{R}$ and $\omega : E \mapsto \mathbb{R}$ be vertex and edge weights. Their extension to sets is $c(V') = \sum_{v \in V'} c(v)$ and $\omega(E') = \sum_{e \in E'} \omega(e)$ for vertex sets V' and edge sets E' .

The *graph partitioning problem* (GPP) asks for a partition of the vertex set V into k equally sized sets. More formally let $k \in \mathbb{N}$ be the desired number of blocks and let $\epsilon \geq 0$ be a hyper-parameter called *imbalance*. GPP then asks for a partition $V = V_1 \cup \dots \cup V_k$ such that $\forall i \neq j : V_i \cap V_j = \emptyset$ and each V_i adheres to the balance constraint, that is $c(V_i) \leq L_{\max} := (1 + \epsilon) \frac{c(V)}{k}$. Such a partition is called a *k-way partition* of G . Let $E_{ij} = \{\{u, v\} \in E \mid u \in V_i, v \in V_j\}$ be the edges crossing between block V_i and V_j . The *edge-cut* of a partition is the total weight of edges crossing between blocks, i.e., $\sum_{i < j} \omega(E_{ij})$. The goal of GP is to determine a balanced k -way partition that minimizes the edge-cut.

A parallel application consists of n weighted tasks which communicate with each other. This is captured by the communication matrix $\mathcal{C} \in \mathbb{R}^{n \times n}$, where an entry C_{ij} denotes the communication volume between tasks i and j . An entry $C_{ij} = 0$ denotes that the tasks do not communicate with each other. Most modern parallel applications only have a very sparse communication pattern between the tasks, which is why we model the communication matrix \mathcal{C} as a task graph $G_{\mathcal{C}}$. For each non-zero entry C_{ij} the task graph has one forward and backward edge with weight C_{ij} .

Let k be the number of PEs on a supercomputer. The cost of communication between the PEs is captured by the hardware topology matrix $\mathcal{D} \in \mathbb{R}^{k \times k}$. An entry \mathcal{D}_{xy} denotes a multiplicative cost factor that is applied to communication between PEs x and y . The cost of task i and j communicating, if placed on PEs x and y respectively, is $C_{ij} \mathcal{D}_{xy}$.

The focus of this work is to tackle the *general process mapping problem*. It asks to assign the vertices of the task graph $G_{\mathcal{C}}$ to PEs of the supercomputer such that the amount of work on each PE is balanced and the total cost of communication is minimized. More formally, we ask for a mapping

$\Pi : [n] \mapsto [k]$ such that $J(C, \mathcal{D}, \Pi) := \sum_{i,j} C_{ij} \mathcal{D}_{\Pi(i)\Pi(j)}$ is minimized, while adhering to the balance constraint.

In the *hierarchical process mapping problem* (HPMP), a special variant of the GPMP, the hardware topology of the supercomputer is described by a homogeneous *hierarchy* $H = a_1 : \dots : a_\ell$. It denotes that each processor has a_1 PEs, each node has a_2 processors, each rack has a_3 nodes, and so forth. In total, the system has $k = \prod_{1 \leq \ell} a_i$ PEs. Corresponding to the hierarchy, a distance $D = d_1 : \dots : d_\ell$ is given which denotes the cost factor between the PEs. Two PEs on the same processor have a cost factor of d_1 , two PEs on the same node but on different processors have a cost factor of d_2 and so forth.

In GPMP we typically assume $n > k$, i.e., we have (considerably) more tasks than PEs. If $n = k$ the problem is known as the *one-to-one process mapping problem* (OPMP) which is identical to the *quadratic assignment problem* (QAP). The QAP is commonly solved using refactorization and linearization techniques [2], [3], [21], of its corresponding mixed integer linear programming formulation [30]. We refer the reader to [4], [9], [32] for comprehensive surveys. The problems GPP, GPMP, HPMP and QAP are all NP-hard problems [17], [39] and no constant factor approximation guarantee exists unless P = NP.

B. Multilevel Graph Partitioning

Modern graph partitioning relies on the multilevel approach, which works in three phases, coarsening, partitioning and uncoarsening with refinement. In the *coarsening* phase a succession of smaller graphs G, G_1, \dots, G_t is computed, with the goal that a smaller graph G_{i+1} retains the same overall structure as G_i . A “good” partition of G_{i+1} would then also resemble a “good” partition for G_i . Coarsening is applied until the coarsest graph has less than ck vertices, where c is a tunable constant. To coarsen a graph, one usually applies a matching or a clustering algorithm. The matching algorithm rates each edge and then determines a maximum weighted matching. Edge contraction is then applied on the determined matching. Edge contraction on an edge $\{u, v\}$ is applied by replacing vertices u and v with a new vertex w with weight $c(w) = c(u) + c(v)$. Former neighbors of u and v are connected to w with the same edge weight. Parallel edges are fused and their weight is summed. A clustering algorithm first determines clusters in the graph, and then contracts each cluster into one super-vertex. The vertex weights and parallel edges are handled in the same way as in the matching.

In the *initial partitioning phase*, the coarsest graph G_t is partitioned. Since G_t is very small, expensive but high-quality algorithms, such as recursive bisection or direct k -way partitioning, can be applied to minimize edge-cut.

The *uncoarsening and refinement* phase iteratively uncontracts the graphs G_{i+1} into G_i by undoing the contractions. After each uncontraction, local search algorithms are applied to improve the objective. The algorithms try to move vertices across the blocks to minimize the edge-cut, while respecting the balance constraint. Widely used refinement algorithms are

the Fiduccia-Mattheyses (FM) algorithm [16], label propagation [38] and flow-based refinement [40]. Notable serial graph partitioners are METIS [27], KAFFPA [40], JOSTLE [48], SCOTCH [36] and KAHYPAR [41].

III. RELATED WORK

Process mapping is closely related to graph partitioning, which has already seen a tremendous amount of research over the last few decades. We already gave a brief overview in Section II-B and refer the reader to [6], [8], [10], [42] for more comprehensive surveys. We will here give an overview of JET [18], a GPU-based graph partitioning (Section III-A), and of process mapping (Section III-B).

A. GPU Multilevel Graph Partitioning

Gilbert et al. [18] present JET, a GPU-accelerated multilevel graph partitioner designed to achieve high partition quality and fast runtimes. Their main contribution includes a novel GPU-parallel refinement algorithm based on label propagation [38]. They implemented their algorithm in the performance-portable Kokkos framework [14], enabling execution on GPUs and multi-core CPUs with a single code base.

Matching. JET utilizes a two-hop matching [29], originally developed for MT-METIS [28], a shared-memory graph partitioner. The algorithm first applies a standard heavy-edge matching and only if more than 25% of vertices remain unmatched a two hop-matching is applied. A heavy edge-matching determines for each vertex its heaviest edge and two neighbors are matched if they agree on their heaviest edge. The two-hop matching can be split into three categories: *leaf*, *twin* and *relative* vertices. Leaf vertices have degree one, two twin vertices share the same neighborhood and relative vertices share at least one common neighbor. To identify twin vertices the neighborhoods of all vertices are hashed and sorted, so vertices with the same neighborhood can easily be found. To accelerate the matching of relatives, special matchmaker vertices with small degree are used. The two-hop matching first matches leaf vertices that share a neighbor, then twin vertices and in the end relative vertices, if necessary.

Coarsening. To coarsen the graph, a fine-grained per vertex hashing algorithm is deployed. First the maximum neighborhood size of each vertex in the coarse graph is overestimated. Then a prefix-sum over the sizes is determined, assigning each vertex a subarray to store its neighbors. Each vertex hashes its new neighboring vertices and inserts them and their weight into their respective subarray. In the end, the edges of all vertices are extracted into the classic Compressed Sparse Row (CSR) format.

Initial Partitioning. After coarsening to $4k-8k$ vertices, the partitioning of the coarsest graph is delegated to METIS [27] on the CPU. The transfer overhead between CPU and GPU is negligible due to the small size of the coarsest graph.

Refinement. The novel improvement of JET is its refinement algorithm, which alternates between a highly parallelized label propagation [38] algorithm and two rebalancing strategies. A standard serial label propagation algorithm visits the

vertices in random order. A vertex is moved to a neighboring block if it improves the edge-cut and adheres to the balance constraint. This is often repeated in multiple rounds to further refine the partition. However, the local search can get stuck in local optima as only positive moves are allowed. Additional problems arise with parallelization. Moving multiple vertices at once makes it difficult to maintain the balance constraint. Additionally, while each individual vertex move might have a positive impact, moving adjacent vertices in parallel can worsen the solution quality.

Gilbert et al. [18] tackle these problems by splitting the refinement into two parts, first unconstrained label propagation and afterwards rebalancing. The unconstrained label propagation starts by determining for each vertex v the gain $F(v)$ (decrease in edge-cut) of moving it in an adjacent block. All potential vertex moves are then passed through the first filter $F(v) \geq 0 \vee -F(v) < \lfloor c \cdot \text{conn}(v, \Pi(v)) \rfloor$. Here, $\text{conn}(v, b)$ is the sum of edge weights from vertex v to block b . To pass the first filter a move needs to be non-negative (first condition) or its increase in edge-cut must be comparatively small (second condition). The constant $c \in [0, 1]$ controls the number of negative gain moves. These moves are allowed to escape local minima. All moves that pass the first filter are collected in a list \mathcal{X} , which is implicitly sorted decreasingly by gain. For each vertex $v \in \mathcal{X}$, the algorithm then recomputes the gain $F_2(v)$ under an approximate future partition state: if a neighbor u appears earlier in the ordering, it is assumed to have already moved to its new block. In a second filter only the vertices $v \in \mathcal{X}$ with a non-negative gain $F_2(v)$ are moved to their respective destination. To prevent oscillation each vertex that was moved is locked in the next iteration of unconstrained label propagation.

Rebalancing. Since the unconstrained label propagation phase ignores the balance constraint, an additional rebalancing phase is required. JET implements two similar strategies, weak and strong rebalancing. Weak rebalancing determines for each vertex in an oversized partition a the loss of moving it to a valid destination block. Valid destination blocks are blocks b with $c(b) \leq \sigma \leq L_{\max}$. The upper bound σ is used instead of L_{\max} to create a small buffer zone, so the block is not overloaded after only one move. For each oversized block a its vertices are approximately sorted increasingly by loss in a list L_a . Then a prefix $L_a^* \subseteq L_a$ is determined such that moving all vertices in L_a^* will balance block a . This minimizes the loss to balance a specific block, however, the destination blocks might become oversized, so another iteration might be necessary. Strong rebalancing reverses the process. Instead of oversized blocks pushing their vertices out, underloaded blocks will pull vertices from oversized blocks. They will only pull so many vertices such they themselves will not become oversized. This often achieves a balanced partition in just one iteration, however the loss is typically greater as in weak rebalancing. In practice, JET applies two iterations of weak rebalancing followed by one iteration of strong rebalancing if necessary.

In total, JET combines its unconstrained label propagation and rebalancing in multiple iterations and keeps the best so-

lution encountered. The algorithm offers comparable solution quality to the well established CPU-based graph partitioner METIS [27], while being up to 20 times faster. Other GPU graph partitioners are GOODARZI ET AL. [19], SPHYNX [1] and G-KWAY [31].

B. Process Mapping

Similar to graph partitioning, process mapping has also seen a tremendous amount of research, and we refer the reader to Hoefler et. al [25] and Pellegrini [37] for broader overviews. Among the first to implement process mapping, was Hatazaki [22] who used graph partitioning to map MPI processes onto hardware topologies. Träff [46] and Yu et. al [49] implemented mapping algorithms for special hardware, namely for the NEC SX-series of parallel vector computers and the Blue Gene/L Supercomputer, respectively.

From a theoretical perspective it seems straightforward that minimizing $J(C, D, \Pi)$ will lead to a more performant algorithm. However, the questions remains if this is also true in practice. Brandfass et. al [7] showed that optimizing the communication cost indeed leads to performance improvements in the context of Computational Fluid Dynamics. Manwade et. al [33] show in a more general context that process mapping algorithms improve the performance of MPI applications.

There are two main methods to solve process mapping, the *two-phase* approach and *integrated mapping*. The two-phase approach first leverages standard graph partitioning to determine a balanced k -way partition with small edge-cut of the task graph G_C . The second phase then determines a 1-to-1 mapping of blocks to the PEs that minimizes the communication cost. Müller-Merbach [35] presented a greedy algorithm to obtain an initial mapping, that served as a basis for many future algorithms. After the mapping phase a potential third refinement phase can be used to determine individual vertex moves that decrease the communication cost. Heider [23] introduced a simple swap algorithm that considers all possible $\mathcal{O}(n^2)$ swaps. This method was iteratively improved by Brandfass et. al [7] by avoiding redundant swaps, and Schulz and Träff [43], by utilizing better data structures and restricting the search space. Notable algorithms using the two-phase approach are GLOBALMULTISECTION [47] and SHAREDMAP [44].

GLOBALMULTISECTION [47] employs a method called *hierarchical multisection* inspired by KAFFPA-MAP [43]. KAFFPA-MAP would first create a balanced k -way partition and then create a communication model graph G_M . This graph has k vertices and edges connecting them if the corresponding k -way partition has edges between the blocks. G_M is then perfectly partitioned alongside the hierarchy $H = a_1 : \dots : a_\ell$, first into an a_ℓ -way partition, then each of the blocks into an $a_{\ell-1}$ -way partition and so forth. This is recursively repeated until k blocks are obtained which represent the k PEs of the system. The mapping of blocks to PEs, and therefore vertices to PEs, can be determined by following the recursive calls. GLOBALMULTISECTION improves the approach by not creating the communication model graph G_M , but instead directly determining an a_ℓ -way partition of G_C and then

recurring on each block. Since no perfect balanced partition is needed, GLOBALMULTISECTION has more freedom to move vertices, resulting in lower communication costs.

SHAREDMAP [44] further decreases the communication cost. It introduces an adaptive imbalance strategy that rescales the imbalance parameter ϵ for each individual partitioning. It guarantees that the final k -way partition is ϵ balanced, and often gives each individual partitioning more space to work with. This results in an overall better mapping with lower communication costs. SHAREDMAP uses KAFFPA [40] as one of its underlying graph partitioners, and it offers state-of-the-art solution qualities for process mapping.

The second approach to solve the GPMP, *integrated mapping*, combines the partitioning and mapping into one algorithm. It leverages the multilevel scheme and the refinement algorithms minimize $J(C, D, \Pi)$. Two prominent algorithm are INTEGRATEDMAPPING [15] and MT-KAHYPAR-STEINER [24].

INTEGRATEDMAPPING [15] uses matching based coarsening to create a smaller representation of the graph. The Global Path Algorithm [34], a 1/2-approximation algorithm, is used to determine a matching of vertices. Instead of using the edge weights as a rating, a special rating function $\exp^*({u, v}) = \omega({u, v})/c(u)c(v)$ from [26] is used. As initial partitioning, the hierarchical multisection approach is used. Refinement strategies include quotient graph refinement [40], k -way FM refinement [40], label propagation [38] and multi-try FM refinement [40]. All refinement methods use the *gain* of a vertex v when moving it from its current block $\Pi(v)$ to a new block b . The gain is defined as follows:

$$G_b(v) = \sum_{u \in N(v)} C_{v,u} (D_{\Pi(v), \Pi(u)} - D_{b, \Pi(u)}). \quad (1)$$

Multiple methods are presented to query the distance $D_{i,j}$ between two PEs i and j . The simplest one saves a matrix with $\mathcal{O}(k^2)$ space and access each distance in $\mathcal{O}(1)$. The other methods, have a considerable lower space complexity, but come with more computational load.

MT-KAHYPAR-STEINER [24] originally was developed to minimize wire lengths in VLSI designs. Logical units, hypergraph \mathcal{H} , are mapped to chip locations, edge-weighted graph \mathcal{C} , such that the total sum of used edge-weights, the implicit wire-length distance, is minimized. Replacing \mathcal{H} with the task graph G_C and \mathcal{C} with the hardware topology matrix D leads to GPMP. MT-KAHYPAR-STEINER is integrated into the shared-memory parallel hypergraph partitioner MT-KAHYPAR [20]. The algorithm follows the multilevel (hyper-)graph partitioning approach. First the hypergraph is clustered, and these clustered are coarsed into a smaller graph. An initial k -way partition of the hypergraph is determined and then greedily mapped onto the chip locations. As local search refinement algorithms, label propagation [38], FM refinement [16] and flow-based refinement [40] are used.

C. Kokkos

We utilize the Kokkos [14] library to implement our algorithms. Kokkos is a C++ library providing performance portability across many-core architectures, including GPUs. It abstracts two main concepts: (1) Parallel execution patterns and (2) Multidimensional arrays. Since multidimensional arrays are not used in this work, we focus on the parallel execution patterns, which are built around three fundamental primitives. (a) *parallel_for* executes N independent work units in parallel. Each work unit operates on the same user defined function $f(i)$ with only the index $i \in [0, N)$ changing for each work unit. (b) *parallel_reduce* performs a reduction $R = \bigoplus_{i=0}^{N-1} f(i)$ over values returned by $f(i)$ using an associative operator \oplus . (c) *parallel_scan* computes an exclusive prefix sum over a range of values i.e. $y_i = \sum_{j=0}^{i-1} f(j)$. All work units share access to memory, and Kokkos provides atomic operations and deterministic reduction mechanisms to prevent race conditions and ensure correctness on many-core architectures.

D. CSR Graph Format

A graph $G = (V, E)$ is typically stored in the Compressed Sparse Row (CSR) format (also referred to as Compressed Row Storage - CRS). The representation consists of an offset array O (also called *row-pointer*) of size $|V|+1$ and two arrays of size $|E|$, one for the edge vertices E_v and one for the edge weights E_w . The edges incident to vertex v are stored in the contiguous range $[O[v], O[v+1])$ of E_v and E_w . Note that the graph is undirected and an edge $\{u, v\}$ is both stored for u and v . This layout naturally supports parallelization across vertices, with each vertex processing its adjacency list independently.

IV. GPU-ACCELERATED PROCESS MAPPING

The main contribution of this work is the development of two GPU-based approaches for solving the hierarchical process mapping problem. Given the close relationship between process mapping and graph partitioning, and the recent success of GPU-based partitioners in achieving faster runtimes, we aim to extend these advantages to process mapping.

Our first algorithm follows the hierarchical multisection approach. It recursively partitions the task graph G_C along the systems hierarchy: first across islands, then racks, and so forth. The final mapping of blocks, and thus vertices, to PEs is obtained by following the recursive calls. The algorithm is presented in Section IV-A.

The second algorithm integrates process mapping directly into a multilevel scheme and is inspired by the GPU-based graph partitioner JET [18] (Section III-A). Its refinement phase has been adapted to employ the new gain equation (Equation 1). Further details are given in Section IV-B.

A. Hierarchical Multisection

The hierarchical multisection approach was first introduced by Kirchbach et al. [47]. It directly exploits the given hierarchy $H = a_1 : \dots : a_\ell$ of the supercomputer to partition the task graph G_C . First, an a_ℓ -way partition of G_C is determined utilizing a graph partitioning algorithm. The resulting a_ℓ blocks,

represent the largest hardware components of the supercomputer (e.g., the islands). Since the graph partitioner minimizes the edge-cut between the blocks, it directly corresponds to minimizing the communication cost across the islands. Then the algorithm recursively partitions each of the a_ℓ blocks into an $a_{\ell-1}$ -way partition. These blocks represent the second-largest component of the system (e.g., racks within islands). Again, minimizing the edge-cut corresponds to minimizing the communication across the racks of each island. This recursive procedure is continued until k blocks are obtained. The mapping of the k blocks to the k PEs can be extracted by following the recursive calls.

Schulz and Woydt [44] improved this method by introducing an adaptive imbalance parameter. Using the original imbalance parameter ϵ for each partitioning can overall result in an unbalanced k -way partition, i.e., some PEs may be overloaded. To avoid this problem, an adaptive imbalance parameter ϵ' is determined for each partitioning. It depends on the original imbalance ϵ , the overall graph weight $c(V)$, the weight of the current subgraph $c(V')$, the desired number of blocks k , the number of total blocks the current subgraph will be partitioned into k' and the depth of the current partition in the hierarchy d . The adaptive imbalance is then determined by

$$\epsilon' = \left((1 + \epsilon) \frac{k' c(V)}{k c(V')} \right)^{\frac{1}{d}} - 1. \quad (2)$$

Using the adaptive imbalance guarantees that the final partition is ϵ -balanced. Experimental results in [44] demonstrate that the adaptive imbalance improves the overall mapping quality. In particular, the SHAREDMAP [44] implementation currently achieves state-of-the-art solution quality for the HPMP.

To adopt the hierarchical multisection approach to GPUs, we must (1) employ a GPU-based graph partitioner and (2) construct the resulting subgraphs directly on the GPU.

For the partitioning step, we use JET [18] which we already presented in Section III-A. JET outperforms CPU-based graph partitioners in terms of speed by factor in the range from 2 to 20 times while delivering equal or better solution quality. Alternative GPU-based graph partitioners such as SPHYNX [1] or G-KWAY [31] could also be used. As no comprehensive comparison between GPU partitioners exists, we adopt JET for its thorough evaluation. However, any faster or higher-quality alternative would translate to our algorithm.

For the second step, we need to build the subgraphs of a graph $G = (V, E)$ given a partition $\Pi : [n] \mapsto [k]$. To circumvent the costly down- and upload between the CPU and GPU, the entire process is executed on the GPU. Our algorithm works in k iterations, where each iteration builds one subgraph G_i . Each iteration consists of three phases. The first phase determines the number of vertices n_i , edges and the subgraphs weight using three *parallel_reduce* loops. A vertex v belongs to the i th subgraph if $\Pi(v) = i$ and likewise an edge $\{u, v\}$ belongs to it, if $\Pi(u) = \Pi(v) = i$. The second phase determines a mapping between the vertices of G_i to the vertices of G_C . The vertices of G_i need to be indexed from 0 to $n_i - 1$, which is also incorporated into the

Algorithm 1 Recursive Hierarchical Multisection

Require: Graph G , Hierarchy $H = a_1 : \dots : a_\ell$

```
1: function HM( $G_L = (V_L, E_L), H, i, I, \Pi_L$ )
2:   if  $i = 0$  then
3:     ID  $\leftarrow$  CALCID( $H, I$ )
4:     for  $v \in V_L$  do  $\Pi(\Pi_L(v)) \leftarrow$  ID
5:      $\epsilon' \leftarrow$  ADAPIMB(...) ▷ uses Eq. 2
6:      $\Pi' \leftarrow$  JET( $G_L, a_i, \epsilon'$ )
7:      $j \leftarrow 0$ 
8:     for  $G'_L \in$  CREATESUBGRAPHS( $G_L, \Pi'$ ) do
9:        $\Pi'_L \leftarrow$  MAPTOG( $G'_L, \Pi_L$ )
10:      HM( $G'_L, H, i - 1, I + [j], \Pi'_L$ )
11:       $j \leftarrow j + 1$ 
12:   end function
13: HM( $G_C, H, \ell, I = \square, \text{IDENTMAP}(G)$ )
```

mappings. The mappings are needed so we can propagate the assigned partition of vertices in G_i back to the vertices of G_C . This step is efficiently implemented via a *parallel_scan* over the vertex set. The prefix sum assigns each vertex a unique new vertex in the range $[0, n - 1)$. In the third phase, we construct the subgraph using a *parallel_scan*. The scan first computes the CSR offsets for each vertex and then writes the corresponding edges and weights. For each vertex u only edges $\{u, v\}$ in the same subgraph are inserted, while the mapping functions translate between global and local vertex IDs. Subgraph creation usually takes less than 2% of the total runtime of the complete algorithm.

Algorithm 1 presents the pseudocode of the hierarchical multisection method. The function takes as input a (sub)graph G_L , the hierarchy H , the current hierarchy level i , an *identifier* list I , and a local mapping Π_L that maps the vertices of G_L to the vertices of G_C . The identifier list I uniquely identifies the position of the subgraph within the system hierarchy. Lines 2 – 4 handle the exit condition: when $i = 0$, the subgraph represents one of the final k blocks and all its vertices are assigned to exactly one of the k PEs. The function CALCID(H, I) determines a unique ID for each identifier I such that neighboring components receive consecutive IDs. The mapping Π_L is used in Line 5 to translate the local vertices back to their original vertices in G_C and for these vertices the mapping is set to the ID.

If the subgraph G_L resides on a higher level ($i > 0$) then further partitioning is required (Lines 6 – 12). First, The adaptive imbalance ϵ' is determined and then JET [18] is utilized to partition G_L into a_i subgraphs via the mapping $\Pi' : V(G_L) \mapsto [a_i]$. For each resulting subgraph G'_L , we determine a local mapping Π'_L from its vertices to G_C (needed in Line 5). The identifier list I is copied and extended by index j to uniquely identifier the subgraph (needed in Line 3). The algorithm then recurses on each subgraph. Finally, the complete algorithm is invoked in Line 14 with the task graph G_C , the hierarchy H , the highest hierarchy level ℓ , an empty identifier list, and the identity mapping for G_C .

B. Integrated Mapping

The second main contribution of this work is an integrated mapping algorithm that incorporates the mapping directly into the graph partitioning. We follow the multilevel approach, but instead of minimizing the edge-cut we optimize $J(C, D, \Pi)$. The multilevel approach, coarsens the graph to a small representation, determines an initial partition and afterwards uncoarsens the graph and refines the mapping. We will detail our methodology for each phase in the next few paragraphs. We closely follow the matching, coarsening, refinement and rebalancing methods used by the GPU-based graph partitioner JET [18] and adapt them to process mapping.

Edge-List Graph Format. Before presenting the multilevel process mapping scheme, we want to present our extended CSR format. As introduced in Section III-D, the CSR representation naturally supports parallelization over vertices, allowing each thread to process a vertex’s adjacency list independently. However, some computations benefit from direct parallelization over edges. In standard CSR, this requires nested parallel loops, first over vertices, then their neighbors, which leads to poor load balancing due to varying vertex degrees, resulting in idle threads on GPUs. To overcome this, we extend the CSR format with an additional array E_u of size $|E|$ that explicitly stores the opposite endpoint of each edge. This edge-centric representation enables flat parallelism over all edges, improving load balance and GPU utilization. We refer to this edge-list representation as \mathbb{E} throughout the rest of this work.

Matching. We utilize the *two-hop matching* presented by LaSalle et. al [29] but make a few changes. It starts with a heavy-edge matching algorithm. Instead of using $\omega(\{u, v\})$ as the weight of the edge, we use the rating function $\exp^{*2}(\{u, v\}) = \frac{\omega(\{u, v\})^2}{c(u)c(v)}$ presented by Holtgrewe et al. [26] and also used in INTEGRATEDMAPPING [15]. Their experiments showed that it lead to improved running times and solution quality in the context of graph partitioning. By looping over \mathbb{E} in parallel, we determine for each vertex v its preferred neighbor $p(v) = u$ as the one with the greatest rating. Adjacent vertices u with $c(v) + c(u) > L_{\max}$ are excluded to prevent an imbalanced initial solution. Afterwards, we determine in parallel for each vertex v if $p(p(v)) = v$, i.e., vertex v prefers $p(v)$ and $p(v)$ prefers v . These vertices are matched to each other. If the vertices have multiple neighbors with the same rating, then it is very unlikely that v and $p(v)$ prefer each other, and we would end up with few matches. We therefore add a small amount of deterministic noise $\eta(\{u, v\})$ onto each rating. The noise breaks the equality and is small enough to not influence the order of two distinct ratings. The matching procedure can be repeated multiple rounds, excluding previously matched vertices. Afterwards, leaf, twin and relative matchings are also applied multiple times if necessary. We adopt the same hashing and matchmaker vertex strategy of JET to improve performance. Instead of matching at least 75% of vertices, we reduce the percentage to 40%. While this leads to more levels in the multilevel framework, it also allows for more chances to refine the partition in the

Algorithm 2 GPU-based Coarsening

Require: Graph G , Mapping M , # Coarse Vertices n_c

- 1: $B \leftarrow \text{ZERO}(n_c)$ ▷ Upper Bounds
- 2: **for** $v \in V$ **do in parallel**
- 3: $B[M(v)] \leftarrow B[M(v)] + |N(v)|$
- 4: $H_v \leftarrow \text{NULL}(|E|)$ ▷ Vertices
- 5: $H_w \leftarrow \text{ZERO}(|E|)$ ▷ Weights
- 6: $O \leftarrow \text{EXCLUSIVEPREFIXSUM}(B)$ ▷ Offsets
- 7: **for** $(u, v, w) \in \mathbb{E}$ **do in parallel**
- 8: **if** $M(u) = M(v)$ **then** **SKIP** ▷ Self-loop discarded
- 9: $\mathcal{I} \leftarrow [O[M(u)], O[M(u) + 1]]$
- 10: $\text{INSERTORLOOKUP}(H_v, H_w, \mathcal{I}, M(v))$
- 11: **return** $\text{EXTRACTCSR}(B, H_v, H_w)$

refinement phase. In our preliminary experiments using greater values lead to drastically worse solution quality.

Coarsening. Edge-contraction, to create the coarsened graph, is based on a fine-grained per-vertex hashing scheme from JET [18]. The pseudocode can be seen in Algorithm 2. Let $G = (V, E)$ be the current graph and let $M : V \mapsto [n_c]$ map each vertex to its coarse counterpart. The value n_c is the number of vertices in the coarse graph. The algorithm first computes an upper bound on the neighborhood size of each coarse vertex by summing the degrees of all vertices assigned to it (Lines 1 – 3). In Line 4 and 5 two hash arrays, H_v and H_w , are allocated that will hold the edges and their weight. The offset array O denotes the index range $O[v]$ to $O[v + 1]$ where the edges of the coarse vertex v are placed. Next all edges $(u, v, w) \in \mathbb{E}$ are processed in parallel. If both endpoints contract to the same vertex, the edge becomes a self loop and is discarded (Line 8). Otherwise we need to insert $(M(v), w)$ into the adjacency of $M(u)$ in the interval \mathcal{I} . Note that adding $(M(u), w)$ into the adjacency of $M(v)$ is handled by the work unit with reverse edge $(v, u, w) \in \mathbb{E}$. Insertion is done in Line 10, which we will explain in the next paragraph. After the parallel loop ends it remains to extract the actual graph from the arrays H_v and H_w . This boils down to determining the true neighborhood sizes of each vertex and extracting the edges by skipping all Null entries in H_v .

The most important part of our fine grained edge-contraction is the INSERTORLOOKUP function in Line 10. To handle concurrent insertions without locks we utilize atomic compare-and-swap (CAS) operations. A CAS operation compares the value at $H_v[j]$ with NULL and only if so swaps $M(v)$ in its place. Regardless if the check succeeded the previous value is returned. This means, if a thread executes a CAS operation on $H_v[j]$ and NULL or $M(v)$ is returned, a slot for $M(v)$ was found. The weight w will be atomically added to $H_w[j]$. Otherwise the thread will continue to cycle through the interval \mathcal{I} . Since we overestimated the neighborhood size of $M(u)$ at least one open slot will be available. To reduce atomic contention on $H_v[j]$, each thread determines $j \in \mathcal{I}$ by hashing $M(v)$ and then cycling through the range if necessary.

Initial Partitioning. Initial partitioning is performed once the last coarsened graph has fewer than $128k$ vertices. Choos-

ing a smaller threshold often resulted in an imbalanced initial partitions from which the algorithm failed to recover. We apply the hierarchical multisection approach explained in Section IV-A to acquire an initial mapping, but execute it entirely on the CPU. At this stage, the graph is sufficiently small that GPU execution offers no runtime advantage. Moreover, even the GPU-based partitioner JET [18] would internally quickly fall back to the CPU-based partitioner METIS [27] when presented with such small graphs. To execute hierarchical multisection, we utilize the CPU-based partitioner KAFFPA [40] in its FAST configuration. Although the STRONG configuration yields higher-quality mappings, its significantly increased runtime would dominate the total execution time, rendering the overall algorithm non-competitive.

Refinement. We adapt the unconstrained label propagation of JET [18] to use $J(C, D, \Pi)$ as the objective function. The corresponding pseudocode is provided in Algorithm 3. The refinement algorithm begins by determining the best target block $\Pi'(v)$ for each vertex v by maximizing the gain $G_b(v)$ (see Equation 1) across all neighboring blocks (Lines 3 – 5).

In JET, a filter is applied that retains only vertex moves satisfying $G_b(v) \geq 0 \vee -G_b(v) < \lfloor c \cdot \text{conn}(v, \Pi(v)) \rfloor$. This criterion is suitable when minimizing the edge-cut, as both $G_b(v)$ and $\text{conn}(v, \Pi(v))$ depend solely on edge weights and are thus directly comparable. In contrast, for process mapping, $G_b(v)$ contains the additional communication factors and is therefore often much smaller than $\text{conn}(v, \Pi(v))$ and varies significantly, depending on v 's connections. This renders the original condition ineffective. We therefore only allow non-negative moves $G_b(v) \geq 0$ to pass the filter, as it performed best in our preliminary experiments. A more sophisticated filtering criterion may further improve solution quality and remains a topic for future work.

In Line 7, vertices passing this filter are inserted into the set \mathcal{X} , which is implemented as a binary array marking selected vertices. The set is implicitly ordered by ord, defined

Algorithm 3 Unconstrained Label Propagation

Require: Graph G , Mapping Π , Is-Locked array L

- 1: $\Pi' \leftarrow \Pi$
- 2: $\mathcal{X} \leftarrow \text{ZERO}(|V|)$
- 3: **for** $v \in V$ **do in parallel**
- 4: **if** $L[v] = 1$ **then** **SKIP** ▷ Vertex locked
- 5: $B \leftarrow \{\Pi(u) \mid u \in N(v)\}$
- 6: $\Pi'(v) \leftarrow \text{argmax}_{b \in B} G_b(v)$
- 7: **if** $G_{\Pi'(v)}(v) \geq 0$ **then** $\mathcal{X}[v] = 1$
- 8: $\mathcal{M} \leftarrow \text{ZERO}(|V|)$ ▷ To-Move array
- 9: **for** $v \in V$ **do in parallel**
- 10: **if** $\mathcal{X}[v] = 1$ and $G_{\Pi'(v)}(v) \geq 0$ **then** $\mathcal{M}[v] = 1$
- 11: $L \leftarrow \mathcal{M}$ ▷ Lock moved vertices
- 12: **return** \mathcal{M}, Π', L

as

$$\text{ord}(u) \begin{cases} < \text{ord}(v) & \text{if } u \in \mathcal{X} \wedge G(u) > G(v), \\ < \text{ord}(v) & \text{if } u \in \mathcal{X} \wedge G(u) = G(v) \wedge u < v, \\ > \text{ord}(v) & \text{otherwise.} \end{cases}$$

Next, all vertex moves in \mathcal{X} are reevaluated under an approximated future mapping state. If a vertex v has a neighbor u scheduled to move to block $\Pi'(u)$ with $\text{ord}(u) < \text{ord}(v)$, then u is assumed to have already moved when recomputing the gain $\mathbb{G}_{\Pi'(v)}(v)$. We mark each vertex $v \in \mathcal{X}$ in a To-Move array \mathcal{M} if it has non-negative gain $\mathbb{G}_{\Pi'(v)}(v)$ (Lines 9–10). To prevent oscillation of vertices, the To-Move array serves as the locked array L for the next iteration (Line 11). The function returns the To-Move array \mathcal{M} the destination mapping Π' and the Locked array L .

Rebalancing. Our rebalancing is also adapted from JET [18]. JET splits its rebalancing into a weak and strong algorithm. The weak rebalancing keeps the loss small, however, it might need multiple iterations to achieve a balanced partition. The strong rebalancing instead often achieves a balanced partition in one iteration, but has a greater loss.

Weak rebalancing starts by determining for each vertex v in an overloaded block, the move with maximum gain (or equally minimum loss) $G_b(v)$ into a neighboring block b that has a weight smaller than the threshold $\sigma \leq L_{\max}$. The threshold σ is chosen such that there is a small deadzone between σ and L_{\max} , so b can take multiple vertices without instantly being overloaded. In our implementation we start with $\sigma = L_{\max} - 0.065L_{\max}$ and gradually lower it throughout the multilevel scheme until at the lowest level we use $\sigma = L_{\max} - 0.005L_{\max}$. We lower it, since the vertex weights are also gradually getting smaller during uncoarsening. Therefore, we can operate on a more fine level and more blocks become eligible. If for a vertex no such neighboring block exists, a random block that fits the threshold is chosen.

Ideally, each block would store all its outgoing vertex moves decreasingly in a list and then a prefix of the list could be chosen, such that the block becomes balanced. This would grant the smallest possible loss based on the current partition. However, since sorting can be expensive on a GPU, we utilize an approximation of the sorted list similar to JET. Each vertex move is assigned a slot in the list $[+, 0, -1, \dots, -10, -20, \dots, -100, -200, \dots, -1000, X]$.

The slot $+$ holds all positive gain moves, the slot X contains all very large negative gain moves and all other slots hold moves with gain $L[i] \geq G_b(v) > L[i+1]$. Note that at first we increase the range by 1, then by 10 and in the end by 100. This gives us an increased resolution for moves with a comparatively small loss, which minimizes the loss when only a few vertices need to be moved. Note that JET also adopts the $+$ and 0 slot and for any negative moves they use $\log_2(-G_b(v))$ to assign a vertex a slot. The approximated list is build in four phases, first by counting how many vertices fall into each slot, allocating enough memory, building a exclusive prefix-sum over the sizes and in the last phase inserting the vertices into their slots. To reduce atomic

Algorithm 4 Overall Refinement Algorithm

Require: Graph $G = (V, E)$, Mapping Π

```

1:  $L \leftarrow \text{ZERO}(|V|)$ 
2:  $\Pi' \leftarrow \Pi$ 
3:  $i \leftarrow 0, i_w \leftarrow 0$ 
4: while  $i < i^{\max}$  do
5:   if  $\text{maxImb}(G, \Pi') \leq L_{\max}$  then
6:      $\mathcal{M}, \Pi'', L \leftarrow \text{UnconLabelProp}(G, \Pi', L)$ 
7:      $i_w \leftarrow 0$ 
8:   else
9:      $L \leftarrow \text{ZERO}(|V|)$  ▷ Reset Locks
10:    if  $i_w < i_w^{\max}$  then
11:       $\mathcal{M}, \Pi'' \leftarrow \text{weakReb}(G, \Pi')$ 
12:       $i_w \leftarrow i_w + 1$ 
13:    else
14:       $\mathcal{M}, \Pi'' \leftarrow \text{strongReb}(G, \Pi')$ 
15:       $i_w \leftarrow 0$ 
16:     $\Pi' \leftarrow \text{move}(\mathcal{M}, \Pi'')$ 
17:    if  $\text{maxImb}(G, \Pi') \leq L_{\max}$  then
18:      if  $J(C, D, \Pi') < J(C, D, \Pi)$  then  $\Pi \leftarrow \Pi'$ 
19:      if  $J(C, D, \Pi') < \phi J(C, D, \Pi)$  then  $i \leftarrow 0$ 
20:    else
21:      if  $\text{maxImb}(G, \Pi') < \text{maxImb}(G, \Pi)$  then
22:         $\Pi \leftarrow \Pi', i \leftarrow 0$ 

```

contention we utilize $\rho = 2$ mini buckets in each slot and a vertex v is assigned its mini bucket by $v \bmod \rho$. As the last step of weak rebalancing a list prefix is chosen for each block b and all vertices in it are moved. The prefix moves at least $c(b) - L_{\max}$ weight, so that the block b becomes balanced.

Since the lists are approximately sorted by their gain, the prefixes have a small combined loss. However, there is no safeguard against the destination blocks becoming overloaded. While the threshold σ helps in preventing this, it does not guarantee it. Therefore, the destination blocks might become overbalanced and another iteration is required.

Strong rebalancing operates in a similar manner to weak rebalancing but reverses the assignment perspective. As before, each vertex v in an overloaded block b identifies an eligible neighboring target block b' that minimizes the loss of moving v . However, instead of storing the vertex moves with the source block b , they are stored in the lists of the corresponding target block b' . Each target block then selects a prefix of moves from its own list, such that it stays balanced after accepting them. After execution, the target blocks are guaranteed to stay balanced, while the source blocks lose weight and are also likely to be balanced. Consequently, strong rebalancing can restore balance in just one iteration. However, target blocks will often move more vertices than necessary, resulting in a higher overall loss compared to weak rebalancing.

Overall Refinement Algorithm. The complete refinement procedure is summarized in Algorithm 4. The algorithm iteratively alternates between unconstrained label propagation and rebalancing (depending on the current imbalance) until

the maximum number of iterations i_w^{\max} is reached. A copy of the mapping Π' is used and the actual mapping Π is only updated if an improvement mapping has been found. The parameter i_w^{\max} controls how many consecutive iterations of weak rebalancing are applied before a single iteration of strong rebalancing is triggered.

In each iteration, if the current partition Π' satisfies the imbalance constraint (Line 5), the algorithm performs unconstrained label propagation to reduce the communication cost (Line 6). Otherwise, the algorithm invokes weak or strong rebalancing to improve the balance (Lines 8 – 15). After each iteration, the partition Π' is updated (Line 16), and the best feasible solution encountered so far is saved.

The process terminates when no significant improvement in either objective quality or balance has been achieved within the iteration limits. The hyperparameter $\phi = 0.999$ specified the minimum relative improvement of $J(C, D, \Pi)$ that has to be achieved in each iteration. We set $i_w^{\max} = 2$ by default, but increase it to 10 in the final refinement stage of the multilevel pipeline to ensure minimal loss while achieving balance. The maximum number of iterations i_w^{\max} is set to $12 + \text{level}$, where level denotes the current level in the coarsening hierarchy (the original graph at level 0, the coarser representation at higher levels). At coarser levels, graphs are smaller, allowing more iterations, but at finer levels, graphs are larger, so each iteration is more computationally expensive.

Additional Data Structure. Determining the gain of moving a vertex to its neighboring blocks is essential for both label propagation and rebalancing. While this information can be obtained by iterating over the neighbors of a vertex, it can be inefficient as a vertex with 100 neighbors might only be connected to two blocks. We employ an additional data structure [18] that enables rapid access to the neighboring blocks. Conceptually, it is similar to the CSR representation of a graph, however, instead of storing edges, it stores the neighboring blocks and their aggregated weight of edges. For each vertex v , we initially allocate memory for $|\{\Pi(u) \mid u \in N(v)\}| + 2$ entries. The additional capacity accounts for potential future vertex moves. Note that this is less memory than JET, which allocates $\min\{k, |N(v)|\}$ per vertex. Whenever a vertex changes its block assignment, we attempt to update its connectivity within the existing memory. We update the connectivity of u to its neighbors v as follows. For each $(u, v, w) \in \mathbb{E}$, we subtract w from v 's connection to $\Pi(u)$. Should the resulting weight drop to 0, then the slot is freed. Next, we add the connectivity to u 's new block $\Pi'(u)$ in v 's connectivity, if $\Pi'(u)$ does not already exist. If this is not possible, because all slots are already occupied, we mark in a bit array, that $\Pi'(u)$ could not be inserted into v 's adjacency. As a last step we add the weights w to the slot $\Pi'(u)$. All these steps utilize a *parallel_for* loop over the edge list \mathbb{E} . If any vertex cannot be updated because not enough slots are available, we trigger a full rebuild of the data structure. Any vertex that exceeded its capacity receives $|\{\Pi(u) \mid u \in N(v)\}| + 2$ slots, while all other vertices retain their slots.

TABLE I
BENCHMARK INSTANCE PROPERTIES.

SuiteSparse			Other		
Graph	$ V $	$ E $	Graph	$ V $	$ E $
cop20k_A	99 843	1 262 244	af_shell9	≈504K	≈8.5M
2cubes_sphere	101 492	772 886	thermal2	≈1.2M	≈3.7M
thermomech_TC	102 158	304 700	nlr	≈4.2M	≈12.5M
cf2	123 440	1 482 229	deu	≈4.4M	≈5.5M
boneS01	127 224	3 293 964	del23	≈8.4M	≈25.2M
Dubcova3	146 689	1 744 980	rgg23	≈8.4M	≈63.5M
bmwera_1	148 770	5 247 616	del24	≈16.7M	≈50.3M
G2_circuit	150 102	288 286	rgg24	≈16.7M	≈132.6M
shipsec5	179 860	4 966 618	eur	≈18.0M	≈22.2M
cont-300	180 895	448 799			
Walshaw					
598a	110 971	741 934	wave	156 317	1 059 331
fe_ocean	143 437	409 593	m14b	214 765	1 679 018
144	144 649	1 074 393	auto	448 695	3 314 611

V. EXPERIMENTAL EVALUATION

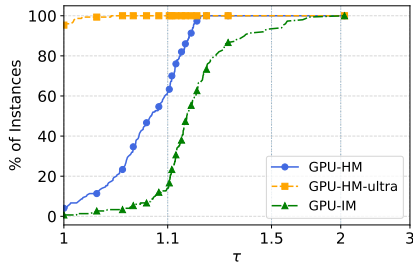
All of our algorithms¹ are implemented in C++ 17 and utilize the Kokkos library [14] version 4.7.0 for the GPU code. It compiles the host side code with GCC 11.4 and the GPU code with Nvidia Cuda compiler 12.6. We use KAFFPA [40] from the KAHIP library version 3.19.0, which is also implemented in C++. We compile with the highest optimization (-O3).

System. The experiments are conducted on a machine that has an Intel® Xeon® w5-3435X, that runs on a max frequency of 3.1Ghz. The system features 128 GB of main memory. The used GPU is a NVIDIA® GeForce RTX™ 4090 with 24GB of memory. It has 16.384 Cuda cores with a boost frequency of 2.5Ghz. The system runs Ubuntu 22.04.4.

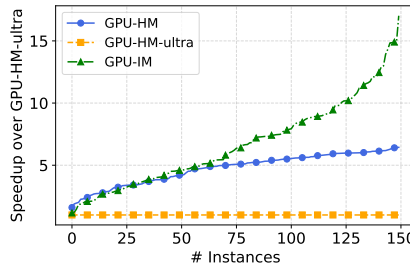
Benchmark Instances. To make our work more comparable, we choose the same benchmark instances as in [15], [24], [43], [44], [47]. They can be seen in Table I. The small instances come from the SuiteSparse Matrix Collection [11]. These represent task graphs from real application. Six graphs were taken from Walshaw's benchmark archive [45], which holds instances for benchmarking graph partitioning algorithms. The graphs *af_shell9*, *thermal2*, *nlr* are from the matrix and numerical section of the 10th DIMACS Implementation Challenge [5]. The graphs *deu* and *eur* are large road networks of Germany and Europe [12]. Graphs *rgg23* and *rgg24* are random geometric graphs with 2^{23} and 2^{24} vertices respectively. Each vertex represents a random point in the unit square, and if their distance is below than $0.55\sqrt{\ln n/n}$ they are connected via an edge. Graphs *del23* and *del24* also have 2^{23} and 2^{24} vertices, with each vertex representing a point in the unit square. The edges are connected such that the graph is Delaunay triangulation.

Experimental Setup. As the hierarchy we choose $H = 4 : 8 : \{1, \dots, 6\}$ and as the distance we choose $D = 1 : 10 : 100$. The imbalance parameter is set to 3% ($\epsilon = 0.03$). Each algorithm is run five times with differ-

¹github.com/HenningWoydt/GPU-HeiProMap



(a) Solution quality



(b) Speedup

Algorithm	Phase	Small	Large
GPU-HM	I/O	24.9%	47.9%
	JET	75.1%	52.1%
GPU-HM-ULTRA	I/O	4.8%	13.7%
	JET	95.2%	86.3%
GPU-IM	I/O	29.3%	74.9%
	Heavy-Edge Matching	0.4%	1.1%
	Edge-Contraction	0.4%	4.7%
	KAFFPA	64.8%	6.2%
	Label Prop. + Bal.	5.0%	12.9%
	Uncoarsening	0.1%	0.2%

(c) Runtime breakdown

Fig. 1. Comparison of solution quality (a) and speedup (b) of our proposed algorithms. Table (c) shows the runtime breakdown per phase.

ent seeds and the *running time* and *communication cost* $J(C, D, \Pi)$ are averaged across the seeds.

Performance Profiles. Performance Profiles [13] enable us to analyze the quality of multiple algorithms. Let \mathcal{A} be the set of all algorithms and let \mathcal{I} be the set of all instances. The quality of algorithm $A \in \mathcal{A}$ on instance $I \in \mathcal{I}$ is $q_A(I)$ and $\text{Best}(I) = \min_{A \in \mathcal{A}} q_A(I)$ denotes the best quality across all algorithms on instance I . For each algorithm A , a performance plot shows the fraction of instances, the y -axis, for which $q_A(I) \leq \tau \text{Best}(I)$, where $\tau \geq 1$ is on the x -axis. For $\tau = 1$ the plot shows the fraction of instances that each algorithm solved with the best solution. Algorithms that perform well have a high fraction of instances solved with minimal τ values, they are towards the top-left corner. Sub-optimal algorithms will have small fractions at minimal τ values, and only achieve higher fractions with greater τ values.

A. Results

We will first analyze the results of our GPU-based hierarchical multisection (GPU-HM) and integrated mapping (GPU-IM) approach. Note that JET [18], which we utilize in GPU-HM, has an ULTRA configuration which executes 18 refinement iterations instead of only one, to improve solution quality. We abbreviated our hierarchical multisection approach that uses JET-ULTRA as GPU-HM-ULTRA. In the end, we will compare our methods against the established algorithms SHAREDMAP [44] and INTEGRATEDMAPPING [15], as they are CPU-based equivalent algorithms to hierarchical multisection and integrated mapping.

Comparison. Figure 1 shows the performance profile (a) and the speedup (b) of our algorithms across all instances. GPU-HM-ULTRA serves as a baseline to measure the speedup as it achieves the lowest communication cost. The default GPU-HM approach reaches a maximum speedup of 6.4 with a geometric mean speedup of 4.4. However, the speedup comes with an increase in communication cost. While the ULTRA variant finds the best solution on 94.7% of instances, GPU-HM does so on only 5.3%. On average, the communication cost of GPU-HM-ULTRA is just 0.1% above the best solution, whereas GPU-HM is 9.3% worse. GPU-IM is the fastest of our algorithms with a maximum speedup of 16 and a geometric mean speedup of 5.6. However, it is also the worst in

terms of communication cost, as it did not achieve the lowest communication cost on any instance and has on average 17.4% higher communication cost than the best solution.

Table 1c reports the percentage of runtime each algorithm spends in its major phases. Results are grouped by graph size: small graphs with fewer than one million vertices and large graphs with more than one million vertices. For the hierarchical multisection approach, most runtime is spent in the partitioning, which gets executed by JET [18]. Only for large graphs does I/O become significant, accounting for 47.9% of the runtime in the case of GPU-HM. The I/O phase includes reading the graph from disk, constructing its data structures, transferring it to the GPU and writing the final partition to disk. Among these steps, loading and constructing the graph dominate the I/O runtime. Overall, reducing the runtime of JET or employing a faster GPU-based partitioner appears to be the most promising direction for improving performance further. The runtime distribution for GPU-IM follows a similar pattern. The greatest runtime percentages are in the phases that do not utilize the GPU, namely I/O and utilizing KAFFPA [40] for the initial partitioning. For smaller graphs, one could coarsen the graph further to partition a smaller graph, which would reduce the required time. However, this often leads to imbalanced solutions and worse communication cost. As later results will show, GPU-IM already lags behind other CPU-based algorithms in terms of solution quality. We therefore utilize GPU-IM as a very fast but low-accuracy algorithm. For larger graphs, the integrated mapping approach spends most of its runtime in the I/O phase.

Comparison to CPU-based Algorithms. We compare our algorithms to the CPU-based solvers SHAREDMAP [44] and INTEGRATEDMAPPING [15], since they performed well in the experimental evaluation of [44]. SHAREDMAP employs the hierarchical multisection approach, just like GPU-HM. For partitioning, it internally uses KAFFPA [40] in either the FAST or STRONG configuration, which trade speed for solution quality. We abbreviate the variants by SHAREDMAP-F and SHAREDMAP-S. INTEGRATEDMAPPING, in contrast, minimizes $J(C, D, \Pi)$ via the multilevel scheme, making it conceptually similar to GPU-IM. It also provides a FAST and STRONG configuration, which we denote by INTMAP-F and INTMAP-S. For comparison, we focus on GPU-HM-ULTRA,

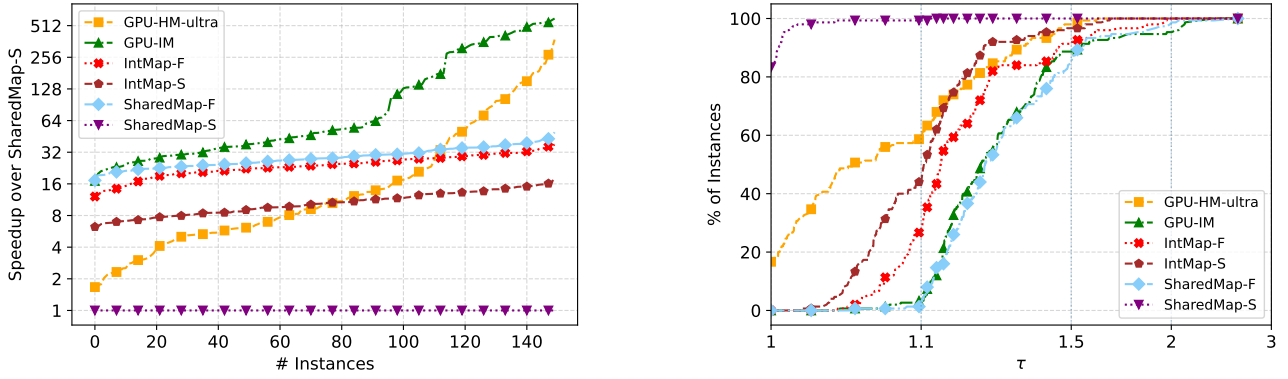


Fig. 2. Comparison of speedup (left) and performance profile of achieved communication costs (right) of our proposed algorithms GPU-HM-ULTRA and GPU-IM to CPU-based algorithms SHAREDMAP and INTEGRATEDMAPPING.

which achieves the highest solution quality, and GPU-IM, which provides the lowest runtime. GPU-HM is omitted for better visual clarity, as its performance lies between the two.

Figure 2 shows the speedup over SHAREDMAP-S (left) and the performance profile (right). Among all algorithms, SHAREDMAP-S achieves the highest solution quality, obtaining the best solution on 125 instances (83.3%). However, this comes at the cost of runtime, as SHAREDMAP-S is also by far the slowest algorithm. GPU-HM-ULTRA finds the best solution on the remaining 25 instances (16.7%). All other algorithms are not able to determine a best solution on any instance. Ranked by average additional cost over the best solution, the algorithms are ordered as follows: SHAREDMAP-S (0.02%), GPU-HM-ULTRA (11.5%), INTMAP-S (14.5%), INTMAP-F (21.1%), GPU-IM (30.7%) and SHAREDMAP-F (31.7%). GPU-IM and SHAREDMAP-F are at most $2.42\times$ and $2.66\times$ worse than the best-known solution, respectively.

In terms of runtime, GPU-IM is the fastest algorithm overall, achieving a maximum speedup of 598.5 and a geometric mean speedup of 77.7 compared to SHAREDMAP-S. While GPU-HM-ULTRA achieves a maximum speedup of 377, its geometric mean speedup is only 13.8. On many instances, it is slower than INTMAP-F/S and SHAREDMAP-F, largely due to the partitioning phase being the bottleneck (see Table 1c). The remaining mean speedups are 28.4 for SHAREDMAP-F, 23.8 for INTMAP-F, and 10.4 for INTMAP-S.

Our algorithms have two clear equal CPU-based counterparts. GPU-HM-ULTRA slightly outperforms INTMAP-S in terms of solution quality. Its geometric mean speedup of 13.8 also exceeds the 10.4 of INTMAP-S, although it is not faster across all instances. Specifically, INTMAP-S is faster on 71% of small instances (speedup of 1.4), whereas GPU-HM-ULTRA dominates on 96% of the large instances (speedup of 5.6). Similarly, GPU-IM is comparable to SHAREDMAP-F in terms of solution quality. On small graphs, it achieves on average 2.6% lower communication costs, while on larger graphs it performs about 2.3% worse. The geometric mean speedup of GPU-IM over SHAREDMAP-F is 1.4 and 10.6 for small and large graphs respectively.

In summary, GPU-HM-ULTRA outperforms the CPU-based algorithm INTMAP-S in both solution quality and running time. However, it cannot reach the state-of-the-art solution quality of SHAREDMAP-S. Nevertheless, GPU-HM-ULTRA is on average an order of magnitude faster. GPU-IM can be almost up to 600 times faster than SHAREDMAP-S, but its solution quality is on average 30.7% higher than the best-known solution.

Comparison to GPU-based Algorithms. While no other GPU-based algorithms currently exist for solving the GPMP, we can compare our algorithms to JET [18]. Note that JET solves the graph partitioning problem, which corresponds to using a distance vector of $D = 1 : \dots : 1$. Since we test the distance $D = 1 : 10 : 100$, JET’s resulting partitions are worse than those of our algorithms. In terms of runtime, however, JET is comparable to GPU-IM as they both follow the multilevel scheme. We base our comparison on the large graph instances (≥ 1 million vertices). Using GPU-IM as the baseline for runtime and communication costs, we observe that JET and JET-ULTRA incur additional communication costs of 42.1% and 38.8% on average respectively. In terms of runtime, JET-ULTRA is comparable to GPU-IM, with a geometric mean speedup of 1.03, whereas JET achieves an average speedup of 1.33. We attribute this performance gap primarily to the 40% matching requirement of our algorithm, compared to the 75% in JET. This allows JET to produce smaller coarse graphs in fewer levels, and thereby reduce runtime. While we could tune our constants for more speed, we observed that it negatively impacted solution quality. Our algorithms GPU-HM and GPU-HM-ULTRA further improve solution quality but are worse in runtime than GPU-IM (see Figure 1), which translates to this GPU comparison.

VI. CONCLUSION

Process mapping assigns vertices of a task graph to the processing elements (PEs) of a supercomputer to balance workload and minimize communication costs. Motivated by the success of GPU-based graph partitioners, we proposed two GPU-accelerated algorithms for this problem.

The first, GPU-HM, applies hierarchical multisection [47] using the GPU-based partitioner JET [18]. The second, GPU-IM, integrates process mapping directly into a multilevel framework, adapting JET's label propagation and rebalancing. GPU-HM-ULTRA achieves up to $300\times$ speedups and is on average a magnitude faster than the state-of-the-art SHAREDMAP [44], with only 11.5% higher communication costs and therefore outperforming INTMAP-S [15]. GPU-IM delivers extreme speedups (mean $77.7\times$, max $598.5\times$) at lower solution quality, however it still outperforms the FAST configuration of SHAREDMAP. Future work will focus on improving solution quality without sacrificing performance e.g., enhancing label propagation filters, refining coarsening and initial partitioning, and exploring more efficient GPU-based partitioners.

REFERENCES

- [1] Seher Acer, Erik G. Boman, and Sivasankaran Rajamanickam. SPHYNX: spectral partitioning for hybrid and accelerator-enabled systems. In *2020 IEEE International Parallel and Distributed Processing Symposium Workshops, IPDPSW 2020, New Orleans, LA, USA, May 18-22, 2020*, pages 440–449. IEEE, 2020.
- [2] Warren P. Adams, Monique Guignard, Peter M. Hahn, and William L. Hightower. A level-2 reformulation-linearization technique bound for the quadratic assignment problem. *Eur. J. Oper. Res.*, 180(3):983–996, 2007.
- [3] Warren P. Adams and Terri A. Johnson. Improved linear programming-based lower bounds for the quadratic assignment problem. In Panos M. Pardalos and Henry Wolkowicz, editors, *Quadratic Assignment and Related Problems, Proceedings of a DIMACS Workshop, New Brunswick, New Jersey, USA, May 20-21, 1993*, volume 16 of *DIMACS Series in Discrete Mathematics and Theoretical Computer Science*, pages 43–75. DIMACS/AMS, 1993.
- [4] Kurt M. Anstreicher. Recent advances in the solution of quadratic assignment problems. *Math. Program.*, 97(1-2):27–42, 2003.
- [5] David A. Bader, Henning Meyerhenke, Peter Sanders, Christian Schulz, Andrea Kappes, and Dorothea Wagner. Benchmarking for graph clustering and partitioning. In *Encyclopedia of Social Network Analysis and Mining*, pages 73–82. 2014. doi:10.1007/978-1-4614-6170-8_23.
- [6] C.E. Bichot and P. Siarry. *Graph Partitioning*. ISTE. Wiley, 2013.
- [7] B. Brandfuss, T. Alrutz, and T. Gerhold. Rank reordering for mpi communication optimization. *Computers & Fluids*, 80:372–380, 2013. doi:10.1016/j.compfluid.2012.01.019.
- [8] Aydin Buluç, Henning Meyerhenke, Ilya Safro, Peter Sanders, and Christian Schulz. Recent advances in graph partitioning. In *Algorithm Engineering - Selected Results and Surveys*, volume 9220 of *Lecture Notes in Computer Science*, pages 117–158. 2016. doi:10.1007/978-3-319-49487-6_4.
- [9] Rainer E. Burkard, Eranda Çela, Panos M. Pardalos, and Leonidas S. Pitoulis. *The Quadratic Assignment Problem*, pages 1713–1809. Springer US, Boston, MA, 1998. doi:10.1007/978-1-4613-0303-9_27.
- [10] Ümit V. Çatalyürek, Karen D. Devine, Marcelo Fonseca Faraj, Lars Gottlieb, Tobias Heuer, Henning Meyerhenke, Peter Sanders, Sebastian Schlag, Christian Schulz, Daniel Seemaier, and Dorothea Wagner. More recent advances in (hyper)graph partitioning. *ACM Comput. Surv.*, 55(12):253:1–253:38, 2023.
- [11] Timothy A. Davis and Yifan Hu. The university of florida sparse matrix collection. *ACM Trans. Math. Softw.*, 38(1):1:1–1:25, 2011. doi:10.1145/2049662.2049663.
- [12] Daniel Dellinger, Peter Sanders, Dominik Schultes, and Dorothea Wagner. Engineering route planning algorithms. In *Algorithmics of Large and Complex Networks - Design, Analysis, and Simulation [DFG priority program 1126]*, volume 5515 of *Lecture Notes in Computer Science*, pages 117–139. Springer, 2009. doi:10.1007/978-3-642-02094-0_7.
- [13] Elizabeth D. Dolan and Jorge J. Moré. Benchmarking optimization software with performance profiles. *Math. Program.*, 91(2):201–213, 2002. doi:10.1007/s101070100263.
- [14] H. Carter Edwards, Christian R. Trott, and Daniel Sunderland. Kokkos: Enabling manycore performance portability through polymorphic memory access patterns. *J. Parallel Distributed Comput.*, 74(12):3202–3216, 2014.
- [15] Marcelo Fonseca Faraj, Alexander van der Grinten, Henning Meyerhenke, Jesper Larsson Träff, and Christian Schulz. High-Quality Hierarchical Process Mapping. In *18th International Symposium on Experimental Algorithms (SEA 2020)*, volume 160 of *Leibniz International Proceedings in Informatics (LIPIcs)*, pages 4:1–4:15. Dagstuhl, Germany, 2020. Schloss Dagstuhl – Leibniz-Zentrum für Informatik. doi:10.4230/LIPIcs.SEA.2020.4.
- [16] Charles M. Fiduccia and Robert M. Mattheyses. A linear-time heuristic for improving network partitions. In *Proceedings of the 19th Design Automation Conference, DAC '82, Las Vegas, Nevada, USA, June 14-16, 1982*, pages 175–181. ACM/IEEE, 1982. doi:10.1145/800263.809204.
- [17] M.R. Garey, D.S. Johnson, and L. Stockmeyer. Some simplified np-complete graph problems. *Theoretical Computer Science*, 1(3):237–267, 1976. doi:10.1016/0304-3975(76)90059-1.
- [18] Michael S. Gilbert, Kamesh Madduri, Erik G. Boman, and Siva Rajamanickam. Jet: Multilevel graph partitioning on graphics processing units. *SIAM J. Sci. Comput.*, 46(5):700, 2024.
- [19] Bahareh Goodarzi, Farzad Khorasani, Vivek Sarkar, and Dhruvjayoti Goswami. High performance multilevel graph partitioning on GPU. In *17th International Conference on High Performance Computing & Simulation, HPCS 2019, Dublin, Ireland, July 15-19, 2019*, pages 769–778. IEEE, 2019.
- [20] Lars Gottlieb, Tobias Heuer, Peter Sanders, and Sebastian Schlag. Scalable shared-memory hypergraph partitioning. In *Proceedings of the Symposium on Algorithm Engineering and Experiments, ALENEX 2021, Virtual Conference, January 10-11, 2021*, pages 16–30. SIAM, 2021. doi:10.1137/1.9781611976472.2.
- [21] Peter M. Hahn, Yi-Rong Zhu, Monique Guignard, William L. Hightower, and Matthew J. Saltzman. A level-3 reformulation-linearization technique-based bound for the quadratic assignment problem. *INFORMS J. Comput.*, 24(2):202–209, 2012.
- [22] Takao Hatazaki. Rank reordering strategy for MPI topology creation functions. In *Recent Advances in Parallel Virtual Machine and Message Passing Interface, 5th European PVM/MPI Users' Group Meeting, Liverpool, UK, September 7-9, 1998, Proceedings*, volume 1497 of *Lecture Notes in Computer Science*, pages 188–195. Springer, 1998. doi:10.1007/BFb0056575.
- [23] Charles H. Heider. A computationally simplified pair-exchange algorithm for the quadratic assignment problem. 1972.
- [24] Tobias Heuer. A direct k -way hypergraph partitioning algorithm for optimizing the steiner tree metric. In *Proceedings of the Symposium on Algorithm Engineering and Experiments, ALENEX 2024, Alexandria, VA, USA, January 7-8, 2024*, pages 15–31. SIAM, 2024. doi:10.1137/1.9781611977929.2.
- [25] Torsten Hoefler, Emmanuel Jeannot, and Guillaume Mercier. *An Overview of Process Mapping Techniques and Algorithms in High-Performance Computing*. 06 2014.
- [26] Manuel Holtgrewe, Peter Sanders, and Christian Schulz. Engineering a scalable high quality graph partitioner. In *24th IEEE International Symposium on Parallel and Distributed Processing, IPDPS 2010, Atlanta, Georgia, USA, 19-23 April 2010 - Conference Proceedings*, pages 1–12. IEEE, 2010.
- [27] George Karypis and Vipin Kumar. A fast and high quality multilevel scheme for partitioning irregular graphs. *SIAM Journal on Scientific Computing*, 20(1):359–392, 1998. doi:10.1137/S1064827595287997.
- [28] Dominique Lasalle and George Karypis. Multi-threaded graph partitioning. In *27th IEEE International Symposium on Parallel and Distributed Processing, IPDPS 2013, Cambridge, MA, USA, May 20-24, 2013*, pages 225–236. IEEE Computer Society, 2013. doi:10.1109/IPDPS.2013.50.
- [29] Dominique LaSalle, Md. Mostofa Ali Patwary, Nadathur Satish, Narayanan Sundaram, Pradeep Dubey, and George Karypis. Improving graph partitioning for modern graphs and architectures. In Antonino Tumeo, John Feo, and Oreste Villa, editors, *Proceedings of the 5th Workshop on Irregular Applications - Architectures and Algorithms, IA3 2015, Austin, Texas, USA, November 15, 2015*, pages 14:1–14:4. ACM, 2015.

- [30] Eugene L. Lawler. The quadratic assignment problem. *Management Science*, 9(4):586–599, 1963.
- [31] Wan-Luan Lee, Dian-Lun Lin, Tsung-Wei Huang, Shui Jiang, Tsung-Yi Ho, Yibo Lin, and Bei Yu. G-kway: Multilevel gpu-accelerated k-way graph partitioner. In Vivek De, editor, *Proceedings of the 61st ACM/IEEE Design Automation Conference, DAC 2024, San Francisco, CA, USA, June 23-27, 2024*, pages 105:1–105:6. ACM, 2024.
- [32] Eliane Maria Loiola, Nair Maria Maia de Abreu, Paulo Oswaldo Boaventura Netto, Peter Hahn, and Tania Maia Querido. A survey for the quadratic assignment problem. *Eur. J. Oper. Res.*, 176(2):657–690, 2007.
- [33] K. B. Manwade and D. B. Kulkarni. Clustmap: A topology-aware mpi process placement algorithm for multi-core clusters. In Subhash Bhalla, Vikrant Bhateja, Anjali A. Chandavale, Anil S. Hiwale, and Suresh Chandra Satapathy, editors, *Intelligent Computing and Information and Communication*, pages 67–76, Singapore, 2018. Springer Singapore.
- [34] Jens Maue and Peter Sanders. Engineering Algorithms for Approximate Weighted Matching. In Camil Demetrescu, editor, *Experimental Algorithms, 6th International Workshop, WEA 2007, Rome, Italy, June 6-8, 2007, Proceedings*, Lecture Notes in Computer Science, pages 242–255. Springer. doi:10.1007/978-3-540-72845-0_19.
- [35] Heier Müller-Merbach. *Optimale Reihenfolgen*. Springer-Verlag, 1970.
- [36] François Pellegrini and Jean Roman. Scotch: A software package for static mapping by dual recursive bipartitioning of process and architecture graphs. In Heather Liddell, Adrian Colbrook, Bob Hertzberger, and Peter Sloot, editors, *High-Performance Computing and Networking*, pages 493–498, Berlin, Heidelberg, 1996. Springer Berlin Heidelberg.
- [37] François Pellegrini. *Static Mapping of Process Graphs*, pages 115–136. John Wiley and Sons, Ltd, 2013. doi:10.1002/9781118601181.ch5.
- [38] Usha Nandini Raghavan, Réka Albert, and Soundar Kumara. Near linear time algorithm to detect community structures in large-scale networks. *Phys. Rev. E*, 76:036106, Sep 2007. doi:10.1103/PhysRevE.76.036106.
- [39] Sartaj Sahni and Teofilo Gonzalez. P-complete approximation problems. *J. ACM*, 23(3):555–565, jul 1976. doi:10.1145/321958.321975.
- [40] Peter Sanders and Christian Schulz. Engineering multilevel graph partitioning algorithms. In *Algorithms - ESA 2011 - 19th Annual European Symposium, Saarbrücken, Germany, September 5-9, 2011. Proceedings*, volume 6942 of *Lecture Notes in Computer Science*, pages 469–480. Springer, 2011. doi:10.1007/978-3-642-23719-5_40.
- [41] Sebastian Schlag, Tobias Heuer, Lars Gottesbüren, Yaroslav Akhremtsev, Christian Schulz, and Peter Sanders. High-quality hypergraph partitioning. *CoRR*, abs/2106.08696, 2021.
- [42] Kirk Schloegel, George Karypis, and Vipin Kumar. *Graph partitioning for high-performance scientific simulations*, page 491–541. Morgan Kaufmann Publishers Inc., San Francisco, CA, USA, 2003.
- [43] Christian Schulz and Jesper Larsson Träff. Better process mapping and sparse quadratic assignment. In *16th International Symposium on Experimental Algorithms, SEA 2017, June 21-23, 2017, London, UK*, volume 75 of *LIPICs*, pages 4:1–4:15. Schloss Dagstuhl - Leibniz-Zentrum für Informatik, 2017. doi:10.4230/LIPICs.SEA.2017.4.
- [44] Christian Schulz and Henning Woydt. *Shared-Memory Hierarchical Process Mapping*, pages 18–31. doi:10.1137/1.9781611978759.2.
- [45] Alan J. Soper, Chris Walshaw, and Mark Cross. A combined evolutionary search and multilevel optimisation approach to graph-partitioning. *J. Glob. Optim.*, 29(2):225–241, 2004. doi:10.1023/B:JOGO.0000042115.44455.f3.
- [46] Jesper Larsson Träff. Implementing the MPI process topology mechanism. In *Proceedings of the 2002 ACM/IEEE conference on Supercomputing, Baltimore, Maryland, USA, November 16-22, 2002, CD-ROM*, pages 40:1–40:14. IEEE Computer Society, 2002. doi:10.1109/SC.2002.10045.
- [47] Konrad von Kirchbach, Christian Schulz, and Jesper Larsson Träff. Better process mapping and sparse quadratic assignment. *ACM J. Exp. Algorithmics*, 25:1–19, 2020. doi:10.1145/3409667.
- [48] C. Walshaw and M. Cross. Mesh partitioning: A multilevel balancing and refinement algorithm. *SIAM Journal on Scientific Computing*, 22(1):63–80, 2000. doi:10.1137/S1064827598337373.
- [49] Hao Yu, I-Hsin Chung, and José E. Moreira. Blue gene system software - topology mapping for blue gene/l supercomputer. In *Proceedings of the ACM/IEEE SC2006 Conference on High Performance Networking and Computing, November 11-17, 2006, Tampa, FL, USA*, page 116. ACM Press, 2006. doi:10.1145/1188455.1188576.